

## General Disclaimer

### One or more of the Following Statements may affect this Document

- This document has been reproduced from the best copy furnished by the organizational source. It is being released in the interest of making available as much information as possible.
- This document may contain data, which exceeds the sheet parameters. It was furnished in this condition by the organizational source and is the best copy available.
- This document may contain tone-on-tone or color graphs, charts and/or pictures, which have been reproduced in black and white.
- This document is paginated as submitted by the original source.
- Portions of this document are not fully legible due to the historical nature of some of the material. However, it is the best reproduction available from the original submission.

SQT

# ICASE REPORT

## ELLIPTIC SYSTEMS AND NUMERICAL TRANSFORMATIONS

(NASA-TM-79422) ELLIPTIC SYSTEMS AND  
NUMERICAL TRANSFORMATIONS (Mississippi State  
Univ.) 21 p HC A02/MF A01 CSCL 12A

N78-21940

Unclas  
1976 14062

C. Wayne Mastin

Joe F. Thompson

Report Number 76-14

May 25, 1976

INSTITUTE FOR COMPUTER APPLICATIONS  
IN SCIENCE AND ENGINEERING  
Operated by the  
UNIVERSITIES SPACE RESEARCH ASSOCIATION  
at  
NASA'S LANGLEY RESEARCH CENTER  
Hampton, Virginia



ELLIPTIC SYSTEMS AND  
NUMERICAL TRANSFORMATIONS

C. Wayne Mastin

Institute for Computer Applications in Science and Engineering

and

Mississippi State University

AND

Joe F. Thompson

Mississippi State University

ABSTRACT

Properties of a transformation method which has been developed for solving fluid dynamic problems on general two-dimensional regions are discussed. These include the error in the construction of the transformation and applications to mesh generation. An error and stability analysis for the numerical solution of a model parabolic problem is also presented.

---

This report was prepared as a result of work performed under NASA Contract No. NAS1-14101 while the first author was in residence at ICASE, NASA Langley Research Center, Hampton, VA 23665.

## I. Introduction

In solving boundary value problems in two-dimensional regions, the treatment of curved boundaries has hindered the implementation of finite difference methods. Some have overcome this obstacle by using finite element methods at the expense of greater programming complexity and computation time. Another alternative is to transform the problem to a region where finite difference methods are more suitable. The expense of a desirable computational region is often a more complicated equation, or system of equations, to be solved.

This report will examine the transformations developed by Chu [1] and Thompson et al. [5] and [6] for solving fluid flow problems. The aim here is to examine the basic transformation method and its construction and not the application to any physical problem. In this way an individual with a particular problem may be better equipped to ascertain if this method is well suited for the solution of his problem. The stability analysis for a model parabolic problem is presented in the same spirit.

## II. The Elliptic Systems

Many of the desirable features of these mappings over others which can be constructed derive from the fact that the mapping is obtained as the solution of an elliptic system of partial differential equations. In particular, the mapping will be differentiable at interior points of the region.

Let  $D$  be a bounded region whose boundary, denoted by  $\partial D$ , is the union of a finite number of disjoint closed contours  $C_1, \dots, C_n$ . Now  $D$  is of

connectivity  $n$  and a simply-connected region can be constructed from  $D$  by removing  $n-1$  curves connecting different boundary components. These curves will be called branch cuts. On removing the branch cuts, the resulting region can be mapped by a one-to-one continuous function onto the interior of a rectangle. The mapping can be extended continuously to the closure of  $D$ ,  $\bar{D}$ , such that the extension is one-to-one except on the branch cuts where the mapping is two-to-one. A typical boundary correspondence for a multiply-connected region is given in Figure 1. With the boundary correspondence specified, the following boundary value problem can be stated. Determine functions  $\xi$  and  $\eta$  which satisfy the semilinear system

$$\begin{aligned} \nabla^2 \xi &= f(\xi, \eta) \\ \nabla^2 \eta &= g(\xi, \eta) \quad \text{on } D \end{aligned} \tag{1}$$

and the boundary conditions

$$\begin{aligned} \xi &= \phi(x, y) \\ \eta &= \psi(x, y) \quad \text{on } \partial D. \end{aligned} \tag{2}$$

The functions  $\xi$  and  $\eta$  are solutions of (1) in the following sense. They are to be treated as branches of solutions of (1) defined on a Riemann surface. Thus the endpoints of the branch cuts are given by the boundary correspondence, but the interior points of the cuts are determined by the solution of (1). The questions of existence and uniqueness of solutions of (1) and (2) will not be dealt with here.

Semilinear systems have been studied extensively for regions in the plane. Since the regions of a Riemann surface that appear in this report can be mapped conformally onto a region of the plane, many of the results on semilinear systems are still valid. It will be assumed that  $\partial D$  and the functions  $f$ ,  $g$ ,  $\phi$ , and  $\psi$  possess sufficient smoothness so that a solution of (1) and (2) exists which is differentiable at all but a finite number of boundary points. In addition, the functions  $f$  and  $g$  will be chosen so that the image of any  $(x,y)$  in  $\bar{D}$  belongs to  $\bar{R}$ . This is true if  $f \equiv g \equiv 0$  by the Maximum Principle and, in general, restrictions on the sign of  $f$  and  $g$  outside of  $\bar{R}$  are sufficient for  $\bar{D}$  to map into  $\bar{R}$ .

In order that a transformation method be applicable to the solution of systems of partial differential equations, it is necessary that the Jacobian of the transformation be nonzero on  $D$ . This is the case, as will be shown next, for harmonic mappings of simply and doubly-connected regions.

Let  $D$  be the simply-connected region bounded by the closed contour  $C$ . Decompose  $C$  into four arcs  $K_1, K_2, K_3, K_4$  having only endpoints in common. The ordering and orientation of the arcs is in a counterclockwise fashion around  $C$ . Let  $a$  and  $b$  be real numbers with  $a < b$ .

**Theorem 1.** If  $\xi$  is a harmonic function on the simply-connected region  $D$  and  $\xi = a$  on  $K_1$ ,  $\xi = b$  on  $K_3$ ,  $\xi$  is increasing on  $K_2$ , and  $\xi$  is decreasing on  $K_4$ , then the gradient  $\nabla \xi \neq 0$  on  $D$ .

**Proof:** The proof is based on the Argument Principle. Suppose  $\nabla \xi = 0$  at  $(x_0, y_0) = z_0$  in  $D$ . Since  $D$  is simply-connected, the harmonic function  $\xi$  will have a single-valued harmonic conjugate  $\xi^*$ . The analytic function

$$W(z) = \xi(x, y) + i \xi^*(x, y)$$

will have  $W'(z_0) = 0$ . Let

$$\omega(z) = W(z) - W(z_0) .$$

The function  $\omega$  has a zero of multiplicity at least two at  $z = z_0$ . By the Argument Principle, the change in the argument of  $\omega$  around  $C$  (or a curve in  $D$  arbitrarily close to  $C$  in case  $\omega$  has a zero on  $C$ ) must be at least  $4\pi$ . This contradicts the boundary values of  $\xi$  since  $\xi(x, y) - \xi(x_0, y_0)$  assumes the value zero only twice on  $C$ .

If  $D$  is mapped to a rectangular region  $R$  by harmonic functions  $\xi$  and  $\eta$  with  $K_1, K_2, K_3, K_4$  mapping to the edges of the rectangle in a one-to-one manner, then both  $\nabla \xi$  and  $\nabla \eta$  will be nonzero on  $D$  by Theorem 1. The fact that the Jacobian is nonvanishing for simply-connected regions was mentioned by Godunov and Prokopov [2]. The validity of their argument requires Theorem 1 although this is not stated. There is also the question as to whether their argument, which uses conformal mappings, can be generalized to multiply-connected regions. An alternate proof is given here which can be used for simply and doubly-connected regions. It is clear that the same reasoning can be used to prove that transformations of many regions of higher connectivity have nonvanishing

Jacobians. However, no proof has been attempted for regions of arbitrary connectivity due to the numerous ways of assigning boundary correspondences and branch cuts.

**Theorem 2.** If the simply-connected region  $D$  is mapped to a rectangular region  $R$  by the harmonic functions  $\xi$  and  $\eta$ , then the transformation has a nonvanishing Jacobian on  $D$ .

**Proof:** Let  $z_0 = (x_0, y_0)$  be an arbitrary point of  $D$ . Then  $\nabla\xi \neq 0$  at  $z_0$  and the curve

$$\{(x,y) | \xi(x,y) = \xi(x_0, y_0)\}$$

determines local orthogonal coordinates  $(s,n)$  where  $s$  is the arc length parameter and  $n$  is the normal in the direction of decreasing  $\xi$ . In terms of these local variables, the Jacobian at any point of  $D$  is  $-\xi_n \eta_s$ . Now  $\xi_n$  and  $\eta_s$  are harmonic on  $D$  and  $\xi_n < 0$  since  $\nabla\xi \neq 0$ . The function  $\eta$  assumes its minimum and maximum values on two arcs of  $D$ , say  $K_2$  and  $K_4$ . On  $K_1$  and  $K_3$ ,  $\eta$  is an increasing function of  $s$ . Therefore, except at a finite number of points,  $\eta_s \geq 0$  on  $\partial D$  which implies  $\eta_s > 0$  on  $D$ . This proves that the Jacobian is positive in  $D$ . Interchanging  $K_2$  and  $K_4$  would result in a negative value.

Let  $D$  be a doubly-connected region interior to the contour  $C_1$  and exterior to  $C_2$ . Let  $\eta$  be the harmonic function on  $D$  which assumes the boundary values  $\eta = a$  on  $C_2$  and  $\eta = b$  on  $C_1$  with  $a < b$ . Let the boundary values of  $\xi$  be prescribed such that  $\xi$  increases from some value  $c$  to a larger value  $d$  as  $C_1$  and  $C_2$  are circumscribed in the counterclockwise direction beginning at points  $z_1$  and  $z_2$  on  $C_1$  and  $C_2$ , respectively. Let  $\xi$  be harmonic except on a



branch cut from  $z_1$  to  $z_2$  where there is a jump of  $d - c$  in the value of the function.

Theorem 3. The transformation of the doubly-connected region  $D$  onto the rectangular region  $R$  has a nonvanishing Jacobian on  $D$ .

Proof: The function  $\eta$  is constant on  $C_1$  and  $C_2$ . A simple relation between  $\eta$  and the conformal mapping of  $D$  onto an annular region shows that the gradient of  $\eta$  is nonzero in  $D$  (see Ohtsuka [3, pp. 44-47]). The rest of the proof is similar to the proof of Theorem 2. Local coordinates  $(s, n)$  are introduced so that the Jacobian takes the form  $-\xi_s \eta_n$ . Now  $\eta_n < 0$  on  $D$  and  $\xi_s$  is a single-valued harmonic function on  $D$  which is nonnegative on  $\partial D$ . Thus  $\xi_s > 0$  on  $D$  and  $-\xi_s \eta_n > 0$ .

The transformations of the simply and doubly-connected regions have nonvanishing Jacobians which together with the prescribed boundary correspondence guarantees that the mapping of  $\bar{D}$  to  $\bar{R}$  is one-to-one and onto except on the branch cuts. A direct proof that the harmonic mapping of the doubly-connected region is one-to-one and onto has been given by P. D. Lax (private communication).

The Theorems in this Section are not true for all transformations generated by the system (1). Nevertheless, the scope of our investigation will be broadened to include solutions of (1) and (2) with the additional hypothesis that the Jacobian of the transformation is non-zero on  $D$ . A first step in that direction is a remark on the effect of the functions  $f$  and  $g$  on the transformation. If  $f$  is increased from 0 to a positive function,  $\xi$  becomes subharmonic. Its values in  $D$  are decreased resulting in a transformation with higher resolution near those boundary components where  $\xi$  assumes its maximum and a

movement of the branch cuts of  $\xi$  in the direction of increasing  $\xi$ . If  $f$  is decreased from 0 to a negative function, higher resolution occurs near boundary components where  $\xi$  assumes its minimum and the branch cuts move in the direction of decreasing  $\xi$ . Similar statements hold for  $\eta$  and  $g$ . This concept has been refined by Thompson et al. [6] to produce transformations with high resolution in various subsets of the region.

The inverse transformation from the rectangular region  $R$  to the region  $D$  is also the solution of a system of partial differential equations. In fact, the system (1) is equivalent to the quasilinear elliptic system

$$\begin{aligned} \alpha x_{\xi\xi} - 2\beta x_{\xi\eta} + \gamma x_{\eta\eta} + J^2 [f(\xi,\eta) x_{\xi} + g(\xi,\eta) x_{\eta}] &= 0 \\ \alpha y_{\xi\xi} - 2\beta y_{\xi\eta} + \gamma y_{\eta\eta} + J^2 [f(\xi,\eta) y_{\xi} + g(\xi,\eta) y_{\eta}] &= 0 \end{aligned} \tag{3}$$

where

$$\begin{aligned} \alpha &= x_{\eta}^2 + y_{\eta}^2 \\ \beta &= x_{\xi} x_{\eta} + y_{\xi} y_{\eta} \\ \gamma &= x_{\xi}^2 + y_{\xi}^2 \\ J &= x_{\xi} y_{\eta} - x_{\eta} y_{\xi} \end{aligned}$$

Boundary conditions are obtained from (2) in the form

$$x = \Phi(\xi, \eta)$$

$$y = \Psi(\xi, \eta) \text{ for } (x, y) \text{ on } \partial D.$$

Note that no boundary conditions are imposed on the image of the branch cuts. The values of the functions  $x$  and  $y$  are set equal on any two subsets of  $\partial R$  corresponding to the same branch cut. Thus, there is a Dirichlet condition on part of  $\partial R$  and a periodicity condition on the remainder.

The first application of solutions of (3) was in the construction of irregular curvilinear meshes. The system (3), with  $f \equiv g \equiv 0$ , was solved numerically by Winslow [7] to create a mesh for finite difference calculations. If a square mesh is constructed on  $\bar{R}$ , the image in  $\bar{D}$  will be a curvilinear mesh. All boundary components and branch cuts lie on mesh lines. The curves of the mesh, on which either  $\xi$  or  $\eta$  is constant, is said to generate a curvilinear coordinate system for  $\bar{D}$ . The following list contains various properties of the curvilinear coordinate system and indicates how they are related to the coefficients in (3).

A. Curvature of  $\xi = \text{constant}$ :  $\alpha^{-3/2} |x_{\eta\eta}y_{\eta} - x_{\eta}y_{\eta\eta}|$

B. Curvature of  $\eta = \text{constant}$ :  $\gamma^{-3/2} |x_{\xi\xi}y_{\xi} - x_{\xi}y_{\xi\xi}|$

C. Angle of intersection of  $\xi = \text{constant}$  and  $\eta = \text{constant}$ :  $\text{Arctan} \left( \frac{J}{\beta} \right)$

D. Metric along  $\xi = \text{constant}$ :  $\sqrt{\alpha} |d\eta|$

E. Metric along  $\eta = \text{constant}$ :  $\sqrt{\gamma} |d\xi|$

When creating a mesh for either finite difference or finite element

calculations, the values in C, D, and E often have an effect on the accuracy of the calculations.

### III. Numerical Transformation

In the numerical construction of the transformation, the system (3) is discretized and solved on a rectangular or triangular mesh using non-linear SOR. Assuming that one desired to solve some partial differential equation, or system of equations, on D, those equations would also be written in terms of the variables  $x$  and  $y$ . When the equations (1) are used in this conversion, which has been the case in previous applications, any error in the numerical solution of (3) could produce additional error in the numerical solution of the transformed equations. Examples will now be presented where the error in the construction of the transformation can be analyzed.

Consider the harmonic mapping of the unit disc

$$D = \{(x,y) \mid x^2 + y^2 < 1\}$$

onto the interior of the square

$$R = \{(\xi,\eta) \mid 1 < \xi < 21, 1 < \eta < 21\}.$$

In order to construct the mapping, suppose the system (3) is discretized on a square mesh of width 1. The resulting difference equations are solved at the interior mesh points of  $R$  by SOR iteration. The mesh points on  $\partial R$  were assumed to map to equally spaced points on  $\partial D$ . The generated curvilinear mesh is exhibited in Figure 2.

At the mesh points of  $D$ , the exact solutions of the equations in (1),  $\xi$  and  $\eta$ , would have integer values  $1, \dots, 21$  whenever the solution of (3) is exact. For comparison, the values of  $\xi$ , and hence  $\eta$  by symmetry, were computed from the Poisson Integral Formula at the interior mesh points obtained from the solution of the difference equations. The values of  $\xi$  beginning at the lower left point of the mesh are given in the Table. Due to symmetry, only values in the left half plane are listed. Note that the maximum absolute error occurs near the boundary points where the Jacobian vanishes; that is, the points which map to the vertices of the square. The error given in Figure 2 is normalized by dividing all function values by the width of the square to compare with the following example.

For a second example, a conformal mapping is constructed. Let  $D$  be the annular region

$$D = \{(x,y) \mid 1 < x^2 + y^2 < e^{2\pi}\} .$$

A conformal mapping of  $D$  onto

$$R = \{(\xi,\eta) \mid 0 < \xi < 1, 0 < \eta < 1\}$$

is given by the equations

$$\begin{aligned} \xi(x,y) &= \frac{1}{2\pi} \log (x^2 + y^2) \\ \eta(x,y) &= \frac{1}{2\pi} \arctan \left( \frac{y}{x} \right) . \end{aligned} \tag{4}$$

The transformation was constructed numerically as in the previous example resulting in the mesh of Figure 3. The coordinates of each mesh point in  $D$  were substituted in (4) and these values were compared with the coordinates of the mesh points on  $R$ . It was found

that the greatest error was in the construction of the function  $\eta$  which has a jump across the branch cut. In all cases the constructed values of  $\xi$  at the mesh points of  $D$  were accurate to five significant digits.

It is hoped that these examples will be of some value to anyone planning to use this transformation method to solve a certain problem. At least some estimate of the magnitude of error in the construction of the transformation can be conjectured as well as the effect of branch cuts and boundary points where the Jacobian vanishes.

#### IV. Stability and Discretization Error

The solution of a time dependent system of partial differential equations by an explicit finite difference scheme requires a stability restriction on the size of the time step. If the system of equations is transformed to a rectangular region, the stability analysis must be carried out on the finite difference analogs of the transformed equations. This will be illustrated by outlining the von Neumann stability analysis of the linearized vorticity transport equation with the forward time - central space differencing scheme. Except for the transformation aspect, the following remarks parallel those in Roache [4, pp. 51-53]. Boundary conditions are neglected.

Let  $\omega$  be a function of  $x$ ,  $y$ , and  $t$  which is a solution of the partial differential equation

$$\omega_t = -u \omega_x - v \omega_y + \mu \nabla^2 \omega \quad (5)$$

for  $t > 0$  and  $(x,y)$  in  $D$  where  $u,v,$  and  $\mu$  are constants. Under the transformation (1), the equation (5) becomes

$$\omega_t = \frac{1}{J} (U \omega_\xi + V \omega_\eta) + \frac{\mu}{J^2} (\alpha \omega_{\xi\xi} - 2 \beta \omega_{\xi\eta} + \gamma \omega_{\eta\eta})$$

for  $(\xi,\eta)$  on  $R$  where

$$U = u y_\eta - v x_\eta + \mu J f$$

$$V = v x_\xi - u y_\xi + \mu J g$$

and  $\alpha, \beta, \gamma,$  and  $J$  are as defined in (3). Suppose a first order forward difference on a mesh of width  $\Delta t$  is used for the time derivative and second order central differencing on a square mesh of width  $h$  is used for the spatial derivatives. The value of  $\omega$  at the point  $(jh, kh)$  at time step  $n$  is denoted by  $\omega_{j,k}^n$ . The value at time step  $n+1$  would be given by the difference equation as

$$\begin{aligned} \omega_{j,k}^{n+1} = & \omega_{j,k}^n - \frac{\Delta t}{2hJ} [U (\omega_{j+1,k}^n - \omega_{j-1,k}^n) + V (\omega_{j,k+1}^n - \omega_{j,k-1}^n)] \\ & + \frac{\Delta t \mu}{h^2 J^2} [\alpha (\omega_{j+1,k}^n + \omega_{j-1,k}^n - 2 \omega_{j,k}^n) - 2\beta (\omega_{j+1,k+1}^n + \omega_{j-1,k-1}^n \\ & - \omega_{j+1,k-1}^n - \omega_{j-1,k+1}^n) + \gamma (\omega_{j,k+1}^n + \omega_{j,k-1}^n - 2 \omega_{j,k}^n)]. \end{aligned}$$

The functions  $U, V, \alpha, \beta, \gamma$  are evaluated at  $(jh, kh)$  with the derivatives replaced by the appropriate difference expressions.

Applying the standard von Neumann Fourier analysis to the above difference equation, necessary stability criteria are

$$\Delta t \leq \frac{|J| h}{|U| + |V|} ,$$

and

$$\Delta t \leq \frac{J^2 h^2}{2 |\mu| (\alpha + \gamma)} .$$

Note that unlike the usual stability criteria in Roache [4], the value of  $\mu$  in (5) appears in both stability conditions since it appears in the expressions for  $U$  and  $V$ . Also, the quantities on the right of the inequalities depend on the point  $(jh, kh)$  and the inequalities should be satisfied at each mesh point if the same size time step is used throughout  $R$ . In the case  $D = R$  and the transformation is the identity mapping, the inequalities reduce to the usual conditions for stability of the forward time - central space difference method of solving (5).

A few straightforward observations will now be made concerning the formal discretization error in solving (5). In the expressions for the derivatives

$$\omega_x = \frac{1}{J} (y_\eta \omega_\xi - y_\xi \omega_\eta)$$

$$\omega_y = \frac{1}{J} (x_\xi \omega_\eta - x_\eta \omega_\xi) ,$$

the difference approximation is of order  $h^2$  if there are positive constants  $K$ ,  $M$ , and  $N$  such that



$$\begin{aligned}
|J| &> K \\
\alpha &< MJ^2 \\
\gamma &< NJ^2
\end{aligned}
\tag{6}$$

for all  $h > 0$ . Since  $\beta^2 < \alpha\gamma$ , the inequalities (6) also imply that the difference approximation for

$$\nabla^2 \omega = \frac{1}{J^2} (\alpha \omega_{\xi\xi} - 2\beta \omega_{\xi\eta} + \gamma \omega_{\eta\eta}) + f \omega_{\xi} + g \omega_{\eta}$$

is of order  $h^2$ . Therefore, the above method for solving the linearized vorticity transport equation (5) is first order in time and second order in space whenever (6) holds.

## REFERENCES

- [1] W. H. Chu, Development of a general finite difference approximation for a general domain, Part I: Machine transformation, J. Comp. Phys. 8 (1971), 392-408.
- [2] S. K. Godunov and G. P. Prokopov, The use of moving meshes in gas-dynamical computations, USSR Comp. Math. Math. Phys. 12 (1972), 182-195.
- [3] M. Ohtsuka, Dirichet Problem, External Length and Prime Ends, Van Nostrand Reinhold, New York, 1970.
- [4] P. J. Roache, Computational Fluid Dynamics, Hermosa, Albuquerque, 1972.
- [5] J. F. Thompson, F. C. Thames, and C. W. Mastin, Automatic numerical generation of body-fitted curvilinear coordinate system for field containing any number of arbitrary two-dimensional bodies, J. Comp. Phys. 15 (1974), 299-319.
- [6] J. F. Thompson, F. C. Thames, C. W. Mastin, and S. P. Shanks, Use of Numerically generated body-fitted coordinate systems for solution of the Navier-Stokes equations, Proc. AIAA 2nd Comp. Fluid Dynamics Conf., Hartford, 1975.
- [7] A. M. Winslow, Numerical solution of the quasilinear Poisson equation in a nonuniform triangle mesh, J. Comp. Phys. 2 (1967), 149-172.

Table. Exact values of  $\xi$  for computed difference values of  $(\xi, n)$ .

$\xi \backslash n$	2	3	4	5	6	7	8	9	10	11
2	1.92	1.95	1.97	1.98	1.99	1.99	1.99	1.99	1.99	1.99
3	2.95	2.94	2.95	2.97	2.98	2.98	2.99	2.99	2.99	2.99
4	3.97	3.95	3.95	3.96	3.97	3.98	3.98	3.98	3.99	3.99
5	4.98	4.97	4.96	4.97	4.97	4.98	4.98	4.98	4.98	4.98
6	5.99	5.98	5.97	5.97	5.97	5.98	5.98	5.98	5.98	5.98
7	6.99	6.99	6.98	6.98	6.98	6.98	6.98	6.98	6.99	6.99
8	8.00	7.99	7.99	7.98	7.98	7.99	7.99	7.99	7.99	7.99
9	9.00	8.99	8.99	8.99	8.99	8.99	8.99	8.99	8.99	8.99
10	10.00	10.00	10.00	10.00	9.99	10.00	10.00	10.00	10.00	10.00
11	11.00	11.00	11.00	11.00	11.00	11.00	11.00	11.00	11.00	11.00
12	12.00	12.00	12.00	12.00	12.01	12.00	12.00	12.00	12.00	12.00
13	13.00	13.01	13.01	13.01	13.01	13.01	13.01	13.01	13.01	13.01
14	14.00	14.01	14.01	14.02	14.02	14.01	14.01	14.01	14.01	14.01
15	15.01	15.01	15.02	15.02	15.02	15.02	15.02	15.02	15.01	15.01
16	16.01	16.02	16.03	16.03	16.03	16.02	16.02	16.02	16.02	16.02
17	17.02	17.03	17.04	17.03	17.03	17.02	17.02	17.02	17.02	17.02
18	18.03	18.05	18.05	18.04	18.03	18.02	18.02	18.02	18.01	18.01
19	19.05	19.06	19.05	19.03	19.02	19.02	19.01	19.01	19.01	19.01
20	20.08	20.05	20.03	20.02	20.01	20.01	20.01	20.01	20.01	20.01

REPRODUCIBILITY OF THE  
ORIGINAL PAGE IS POOR

REPRODUCIBILITY OF THE  
ORIGINAL PAGE IS POOR

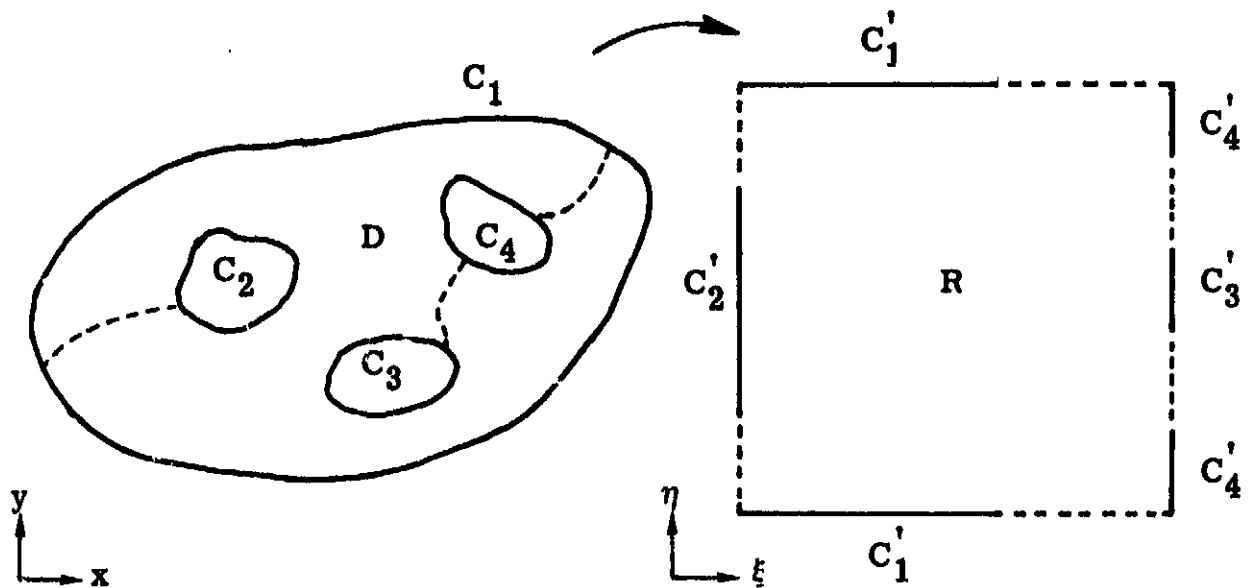
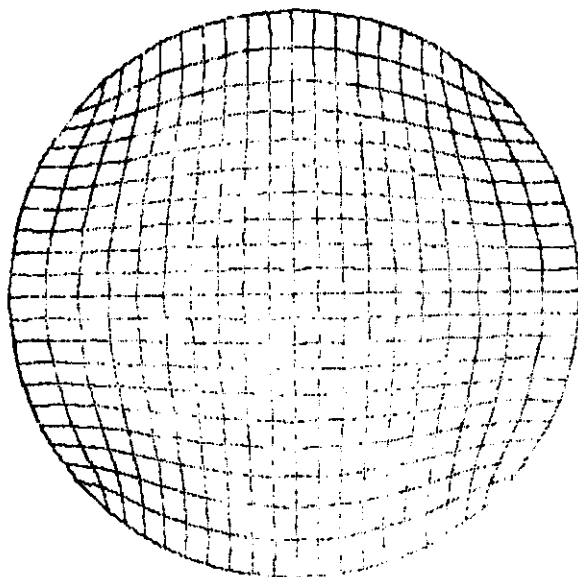


Figure 1. Transformation of a multiply-connected region onto a rectangular region.

<b>Mesh size</b>	<b>Error</b>
<b>21 x 21</b>	<b>0.004</b>



**Figure 2. Curvilinear mesh on a disc and maximum absolute error in mapping to a square of unit width.**

Mesh size	Error
21 x 21	0.01252
42 x 42	0.00290
84 x 84	0.00067

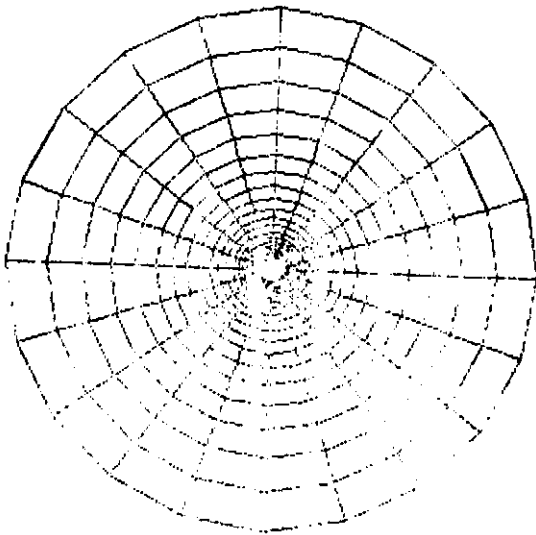


Figure 3. Curvilinear mesh on an annular region and maximum absolute error in mapping to a square of unit width.